Geodesy and Cartography
ISSN 2029-6991 / eISSN 2029-7009
2022 Volume 48 Issue 2: 92–106
https://doi.org/10.3846/gac.2022.14551

UDC 528.24

SELECTION OF AN OPTIMUM GLOBAL GRAVITATIONAL MODEL FOR GEOLOGICAL MAPPING OF AFIKPO AND ANAMBRA BASINS IN NIGERIA

Ojima Isaac APEH[1,2*], Robert TENZER[1]

[1]Department of Land Surveying and Geo-Informatics, Hong Kong Polytechnic University, Hong Kong, Hong Kong
[2]Department of Geoinformatics and Surveying, University of Nigeria, Enugu Campus, Enugu, Nigeria

Received 11 March 2021; accepted 23 May 2022

Abstract. Combined Global Gravitational Models (GGMs) are being used in numerous geoscience applications, most notably for gravimetric geoid modeling (in geodesy) and for geological mapping and geophysical explorations (in the Earth's sciences). The aim of this study is to evaluate the suitability of different combined GGMs that could be used for the geological mapping of middle belt region and Southeastern Nigeria. For this purpose, we digitized geological maps of Afikpo and Anambra Basins to evaluate geological signatures implied by gravity field quantities (Bouguer gravity anomalies and vertical gravity gradient) derived from the EGM2008, EIGEN-6C4, GECO, SGG-UGM-1 and XGM2019e_2159 gravitational models. We also stochastically evaluated the performance of these GGMs by computing their Root-Mean-Square (RMS) fit with ground-based gravity measurements. The results show that the EIGEN-6C4 and XGM2019e_2159 models have the best RMS fit with the ground-based gravity data. A spatial pattern in Bouguer gravity maps (compiled using these two models) generally closely agrees with a geological configuration of the basins, while also exhibiting some more detailed geological features. Interestingly, however, despite the XGM2019e has the best fit and better mimics major geological features, the gravity image from this model does not exhibit a sediment signature in a portion of the Afikpo basin. A possible reason is that the topographic information used to recover a higher-frequency gravity spectrum of this model might suppress a gravitational signature of subsurface density structures. A comprehensive interpretation of geological features thus requires a careful analysis of existing GGMs, terrestrial gravity data as well as all other reliable geological and geophysical information.

Keywords: bouguer/free-air gravity anomalies, geological mapping, GGMs, gravity gradient, gravimetric interpretation.

Introduction

Over the years, geological mapping has mostly relied on *in situ* seismic or geotechnical surveys, which are cost-intensive and time-consuming. Nowadays, Global Gravitational Models (GGMs) are increasingly being used to identify possible lineaments/faults, meso-scale regional geological features or lithological boundaries (Chouhan et al., 2022). These models are also used to interpret lithospheric and crustal structures (Rathnayake & Tenzer, 2019; Ghomsi et al., 2020; Dogru et al., 2018) and to determine the Moho depth (Chen & Tenzer, 2017) and other subsurface structures, such as a sediment basin morphology (Pal & Kumar, 2019; Pal et al., 2016).

The GGM coefficients describe the Earth's external gravitational field. GGMs are either satellite-only or combined, depending on the source(s) of data used for their compilation. Different data sources (satellite, terrestrial, altimetric, seaborne and airborne) acquired through different platforms are optimally combined (yielding combined GGMs) by means of a least-squares analysis in order to enhance the accuracy and resolution of GGMs that is beneficial for their use in various geoscience applications (Barthelmes, 2013; Pavlis, 2006). Nevertheless, it is a well-known fact that the accuracy of GGM depends on omission errors (i.e., errors due to a limited resolution of GGMs) and commission errors (i.e., errors of spherical harmonic coefficients of GGMs attributed to input data uncertainties as well as errors of numerical procedures applied for a compilation of GGMs). Commission errors vary with location. This implies particularly for combined GGMs of which a higher-degree part of gravity spectra depends on availability of terrestrial and airborne gravity

*Corresponding author. E-mail: *ojima.apeh@connect.polyu.hk*

data used to compile these models. These errors obviously increase over regions where gravity measurements are sparse or missing. Hirt et al. (2016), for instance, demonstrated the existence of large inaccuracies of EGM2008 and EIGEN-6C4 models over Antarctica (due to polar gaps of gravity-dedicated satellite missions and a lack of terrestrial and airborne gravity observations).

As mentioned above, satellite-only gravitational models have a limited resolution. The current spatial resolution of these models derived from the GOCE satellite gravity gradiometry is about 80–120 km. As explained already, even combined GGMs compiled to a relatively high spectral resolution complete to a spherical harmonic degree of 2160 (or similar) have a relatively limited accuracy and resolution over large parts of the world where terrestrial and airborne gravity measurements are not available. Higher-degree spherical harmonics of these models have still a relatively low accuracy (Gilardoni et al., 2015). This was demonstrated, for instance, by Odera (2020). He inspected the accuracy of different GGMs for Nairobi in Kenya. Yilmaz et al. (2018) conducted a similar study for Western Anatolia in Turkey, and Apeh et al. (2018) inspected the accuracy of different GGMs for Enugu State in Nigeria. These studies (and many others) indicate that it is necessary to evaluate the performance of different GGMs for a particular region in order to select the one (or more) models that are suitable for that region in terms of their accuracy and resolution as well as their ability to interpret geological features.

The combined GGMs, selected for this study, have a very similar degree of expansion. In this case, the spatial and spectral resolution is not considered, so that we inspected only their accuracy and their reliability to represent features that are important in geoscience studies. In particular, we validated GGMs by means of their possible use in geophysical explorations of subsurface features in the middle belt and Southeastern Nigeria. For this purpose, we used existing geological information and statistical techniques to assess how realistically these models could reproduce major geological features in this study area, important from a point of view of mineral exploration. Our study differs from previous study conducted for Enugu State in Nigeria by Apeh et al. (2018). Here we used a larger study area with a significantly higher number of ground-based gravity data (more than 2900 gravity points compared to only about 60 points). We also incorporated geological information for the analysis and our validation involved the latest GGMs.

Three gravity field quantities, specifically the free-air gravity anomalies, the Bouguer gravity anomalies and the vertical gravity gradient (i.e., second-order derivative of the disturbing potential), that are of a great geophysical importance, were interpreted in the context of geological and tectonic configuration of the study area. The Bouguer gravity anomalies are used for modeling and interpretation of the Earth's inner structure and processes (Bagherbandi & Sjöberg, 2013; Rathnayake et al., 2020). The free-air gravity anomalies are suitable for the interpretation of their spatial correlation with the topography and sub-surface density structures. Compared to the free-air gravity data, the vertical gravity gradient is particularly sensitive to shallower subsurface density features (cf. Pappa et al., 2019; Bouman et al., 2016).

The study is organized into five sections. Input data acquisition and methods are described and explained in Section 1. Geological maps of the Afikpo and Anambra Basins are presented, and their geological formation briefly reviewed in Section 2. Results are shown in Section 3 and discussed in Section 4. The study is summarized, and major findings concluded in the last Section.

1. Materials and methods

This section provides the summary of input data and explains methods applied to compute gravity field quantities using the GGMs coefficients.

1.1. Ground-based gravity data

We used 2,973 ground-based free-air and Bouguer gravity anomalies over the entire study area (see Figure 1). The Nigerian Geological Survey Agency [NGSA] conducted gravity surveys in the middle belt and Southeastern Nigeria in 2008, 2009 and 2011. These gravity surveys were tied to the International Gravimetric System IGSN'71 (Morelli et al., 1972) through the Primary Gravity Network for Nigeria (PGNN) (Osazuwa, 1986). During the gravity surveys, the Lacoste and Romberg (G-512) gravimeter was calibrated along the Northern Nigeria Calibration Line (Osazuwa, 1992), while the scale was calibrated to the Smithsonian meteorological table that could read with an accuracy of about 3 m. The sling psychrometer was used to measure the air temperature while the relative humidity, used in correcting the barometric readings, was determined from the psychrometric chart. Topographic heights of all gravity stations were measured with two FA-181Wallace & Tiernan and one Brunton altimeters. The 1967 Geodetic Reference System was used as the reference ellipsoid to compute the normal gravity values. More details on the instrumentation and how these gravity surveys were carried out, including numerical procedures utilized in computing the free-air and Bouguer gravity anomalies and the associated gravity corrections, can be found on the website of the Nigerian Geological Survey Agency (NGSA, 2017) or in the study by Apeh et al (2018).

1.2. Global gravitational models

The GGMs are available at the website of the International Centre for Global Earth Models (ICGEM) (http://icgem.gfz-potsdam.de/home). The ICGEM is one of the five services coordinated by the International Gravity Field Service (IGFS) of the International Association of Geodesy (IAG) (Barthelmes & Köhler, 2016). In their online calculation service, many gravity field quantities (such as free-air gravity, Bouguer gravity anomaly, gravity gradient, geoid undulation, height anomaly, etc.) can be computed using GGMs of interest (Barthelmes & Köhler, 2016; Ince

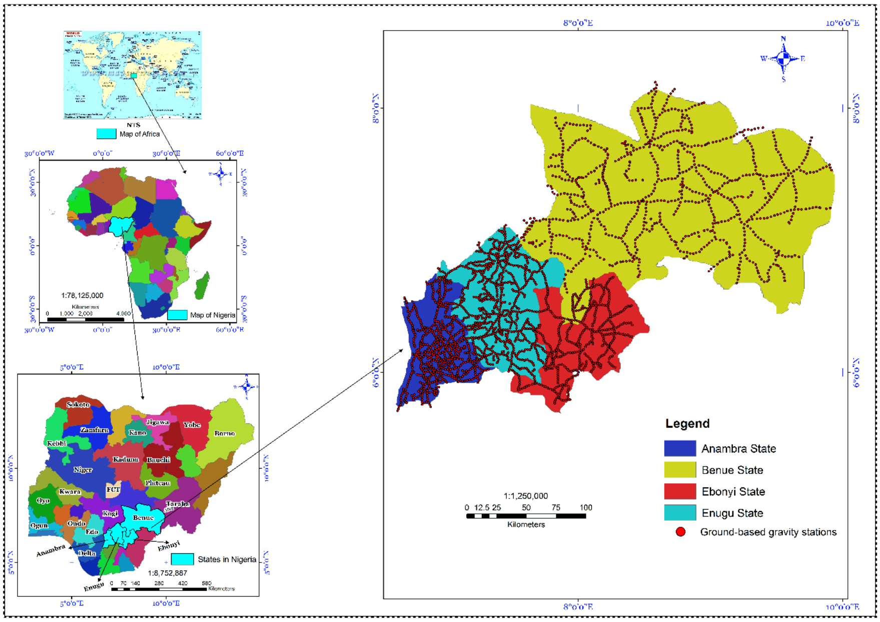

Figure 1. Ground-based gravity stations within the study area

et al., 2019). These gravity field quantities are numerically computed by applying a spherical harmonic expansion of satellite tracking, ground-based gravity, satellite-altimetry and topographic data over the globe (Barthelmes, 2013). In this study, we tested five combined GGMs, namely XGM2019e_2159, SGG-UGM-1, GECO, EIGEN-6C4 and EGM2008 (see Table 1).

Table 1. Summary of the five combined GGMs used in this study

Models (d/o)	Sources of Data	References
XGM2019e_2159 (2190)	A, G, S(GOCO06s), T	Zingerie et al., 2019
SGG-UGM-1 (2159)	EGM2008, S(GOCE)	Liang, 2018 & Xu et al., 2017
GECO (2190)	S(GOCE), EGM2008	Gilardoni et al., 2016
EIGEN-6C4(2190)	A, G, S(GOCE), S(GRACE), S(LAGEOUS)	Förste et al., 2014
EGM2008(2190)	S(GRACE), G, A	Pavlis et al., 2012

Note: Notation used: S = Satellite Tracking Data, G = Gravity Data, A = Altimetry Data, T = Topography, d/o = degree/order.

The XGM2019e_2159 was compiled from the satellite model GOCO06s and by incorporating terrestrial observations in order to recover information about a higher frequency of gravity spectrum. It was augmented with topography-derived gravity over land using the EARTH2014 topographic heights (Hirt & Rexer, 2015) and gravity anomalies over the oceans derived from satellite-altimetry data using the DTU13 model (Zingerie et al., 2019; Kvas et al., 2015; Andersen et al., 2015). The SGG-UGM-1 model was developed from the EGM2008 model, the GOCE satellite gravity gradiometry (SGG) and the satellite-satellite-tracking (SST) observations. This model was compiled with a spectral resolution complete to degree and order of 2159 (Liang, 2018; Xu et al., 2017). The GECO model was developed based on updating the EGM2008 gravity spectrum up to degree/order of 280 from the GO_CONS_GCF_2_TIM_R5 (GOCE) model. In other words, this GOCE model was used to improve the accuracy of EGM2008 model at low-to-medium frequencies (Gilardoni et al., 2016; Brockmann et al., 2014). The EGM2008 was compiled from the ITG-GRACE03S gravitational model and a global set of the area-averaged free-air gravity anomalies obtained from merging available terrestrial, altimetry-derived and airborne gravity datasets (Pavlis et al., 2012; Mayer-Gürr, 2007). The EIGEN-6C4 was compiled from terrestrial and satellite gravity data including also the GOCE satellite gravity-gradiometry data (Drinkwater et al., 2003; Floberghagen et al., 2011) over the entire mission (from November 2009 to October 2013); see Förste et al. (2014).

1.3. Gravity field quantities

We used the free-air and Bouguer gravity anomalies as well as the vertical gravity gradient. These gravity field quantities were computed via the ICGEM online platform (Barthelmes & Köhler, 2016; Ince et al., 2019), while setting essential parameters during the computation to fit the purpose of the study. We maintained the spatial resolution of each model by computing gravity field quantities to a maximum degree of its expansion. The GRS67 reference ellipsoid was used to compute the normal gravity parameters because parameters of this ellipsoid were used to compute the normal gravity values for the ground-based gravity data and associated to the IGSN'71 datum. The constant topographic density of 2670 kg/m^3 was used to compute the Bouguer gravity anomalies while maintaining the model's defined tidal system. Gaussian filtering was not applied, and the zero-degree term was not taken into consideration.

2. Geological and statistical analysis

We geo-referenced and digitized geological maps of the Afikpo (Figure 2) and Anambra (Figure 3) Basins and used them for a comparative assessment of the results obtained from GGM-derived gravity field quantities using GIS tools. We gridded each of basins with a 5′ × 5′ spatial resolution (identical to that used for computing the gravity field quantities). The computation was carried out on the ETOPO1 topographic surface. It is worth mentioning that the ground-based gravity sites do not cover entirely these two basins and most of them are situated along roads. We then assessed how gravity maps reflects the geological and tectonic configuration of the study area.

The Afikpo and Anambra Basins form part of the study area, situated within the middle belt region and Southeastern Nigeria. The Afikpo and Anambra Basins constitute the southeast lower portion of the Benue Trough. Afikpo area is in the Southern Benue Trough, between the Abakaliki anticlinorium (to the northeast) and the Cameroon Hinge Line (to the southeast). This basin is classified as a continuous southeastward extension of the Anambra Basin towards Calabar, a sedimentary succession comprising sediments of Campanian to Early Paleocene occurring within the Eastern limb of the Abakaliki anticlinorium and as a full-fledged basin which comprises Campanian-Maastrichtian-Early Paleocene (Danian) sediments within the eastern flank of the Abakaliki anticlinorium (Okoro & Igwe, 2018; Nwajide, 2013; Amajor, 1987; Cratchley & Jones, 1965).

The geological map of the Afikpo Basin exhibits eight units (the Nkporo, Mamu, Ezeaku and Asu river groups, the Ajali and Nsukka formations, the Niger Delta sediments, and the Precambrian basement) defined from the basin (Upper Campanian-Eocene) some of which

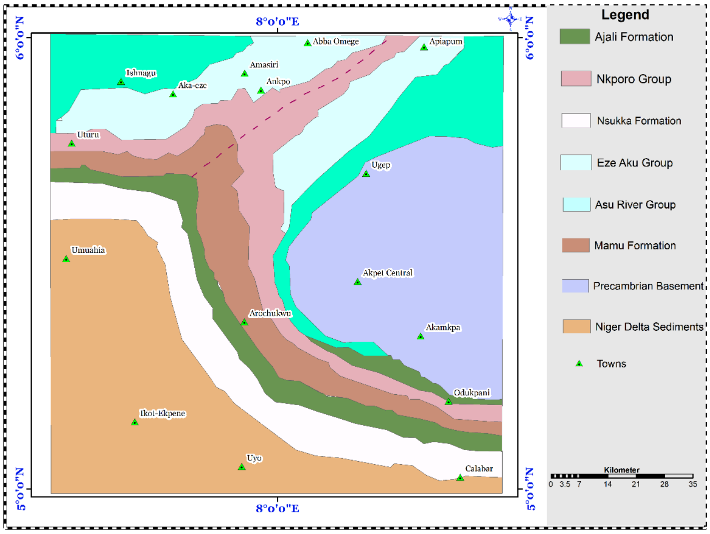

Figure 2. Geological map of the Afikpo Basin (modified after NGSA, 2012)

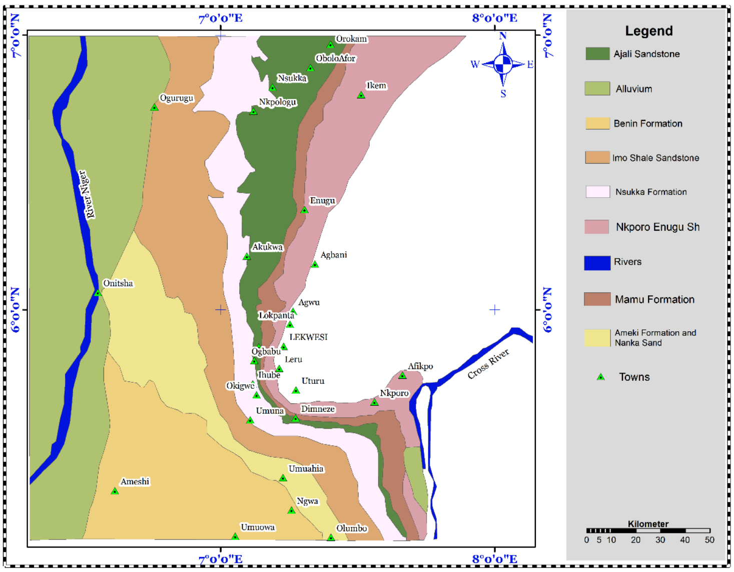

Figure 3. Geological map of the Anambra Basin (modified after Igwe et al., 2013)

are of lateral equivalence. The Campanian-Maestrichtian sequence of the stratigraphic units of the Lower Benue Trough includes the shallow marine of Nkporo Mamu groups and the Ajali and Nsukka formations. During the Turonian and Coniacian times, the Ezeaku group was deposited. The Cretaceous Afikpo sedimentary basin contains the Niger Delta sediments such as fluvial, deltaic and marine rocks. The Asu river group occupies the basal unit of the Abakaliki anticlinorium. The Nsukka formation was initially referred to as the Upper coal measures that overlies the Ajali formation and it is marked by the deposition of carbonaceous shale, sandstones, and some thin coal seams (Cratchley & Jones, 1965; Nwajide, 2013; Ekwere et al., 2012; Okoro & Igwe, 2018).

The Anambra Basin covers an area of about 40,000 km^2 with a sedimentary sequence of 9 km in thickness (Akaegbobi, 2005). Previous studies classified the Anambra Basin by eight geologic formations that include the Benin (Ogwashi-Asaba) formation, Nkporo/Enugu shale, Mamu formation, Ajali sandstone, Nsukka formation, Imo formation, Ameki formation/Nanka sand and Alluvium (e.g., Reyment, 1965; Obi et al., 2001; Igwe et al., 2013; Nwajide, 2013; Anakwuba et al., 2018). The Ameki formation consists of fossiliferous greyish-green sandy clay with calcareous concretions and white clayey sandstones. The Imo formation consists of blue-grey clays and shales and black shales with bands of calcareous sandstone, marl, and limestone. The Benin (Ogwashi-Asaba) formation is mainly characterized by alternation of clays, sands, grits and lignites.

3. Results

In this section, we present gravity and gravity gradient maps and interpret their spatial patterns with respect to the geological configuration of the Afikpo and Anambra basins.

3.1. Ground-based gravity data

Figure 4 illustrates maps of the ground-based and GGM-derived Bouguer gravity anomalies within the study area. We note that the ground-based gravity measurements in the entire study area are relatively sparse. This could

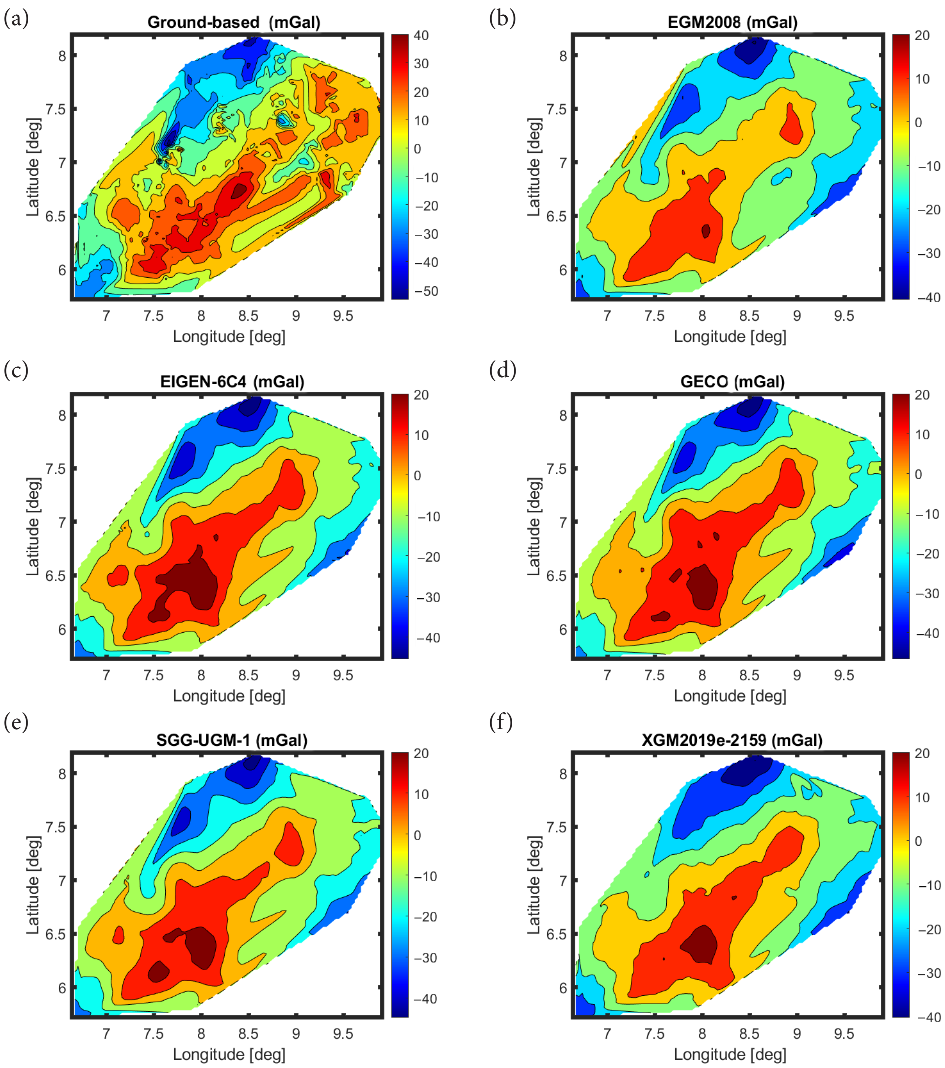

Figure 4. Ground-based versus GGM-derived Bouguer gravity anomalies: a – ground-based; b – EGM2008; c – EIGEN-6C4; d – GECO; e – SGG-UGM-1; and f – XGM2019e

cause some discontinuities in the geological features as portrayed in gravity maps. Figure 5 shows the free-air gravity anomalies. Figure 6 depicts maps of differences between the ground-based and GGM-derived Bouguer gravity anomalies over the study area. The corresponding differences in the free-air gravity anomalies are shown in Figure 7. Statistics of the ground-based and GGM-derived (free-air and Bouguer) gravity anomalies are summarized in Table 2. Statistical summaries of their differences are given in Table 3.

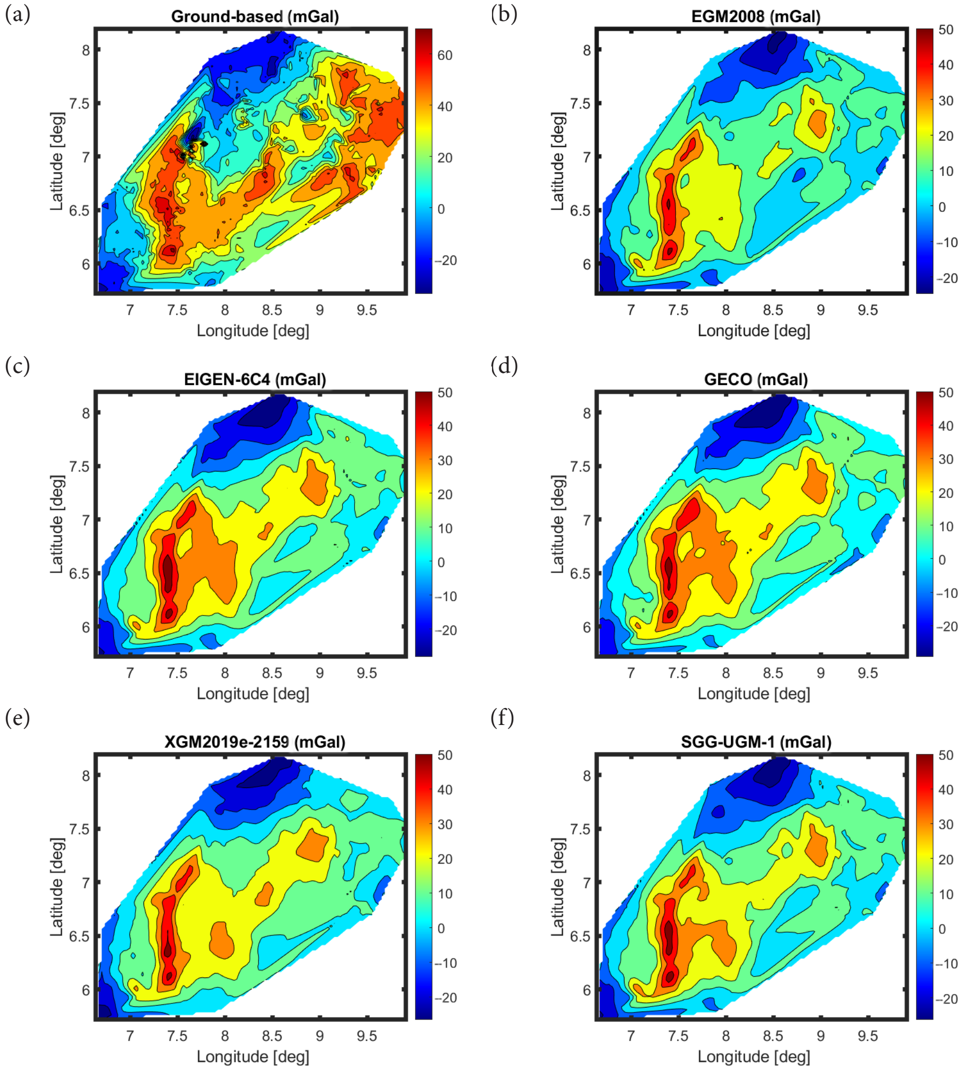

Figure 5. Ground-based versus GGM-derived free-air gravity anomalies:
a – ground-based; b – EGM2008; c – EIGEN-6C4; d – GECO; e – SGG-UGM-1; and f – XGM2019e

Table 2. Statistics of the ground-based and GGM-derived Bouguer and free-air gravity anomalies

Bouguer Gravity Anomalies (mgal)					
	Min	Max	Mean	STD	RMS
Observed	–52.58	43.65	7.17	17.61	0.00
EGM2008	–42.31	21.75	–0.22	11.10	0.00
EIGEN-6C4	–46.71	28.39	1.96	13.52	0.00
GECO	–48.32	27.41	1.35	13.13	0.00
SGG-UGM-1	–46.26	26.78	1.43	12.94	0.00
XGM2019e	–41.27	24.66	1.19	12.39	0.00
Free-air Gravity Anomalies (mgal)					
	Min	Max	Mean	STD	RMS
Observed	–33.98	80.18	26.62	23.40	0.00
EGM2008	–24.77	52.08	16.20	14.29	0.00
EIGEN-6C4	–28.08	56.73	18.36	16.39	0.00
GECO	–29.31	54.24	17.75	16.16	0.00
SGG-UGM-1	–26.24	55.04	17.80	15.63	0.00
XGM2019e	–26.60	54.32	17.59	15.39	0.00

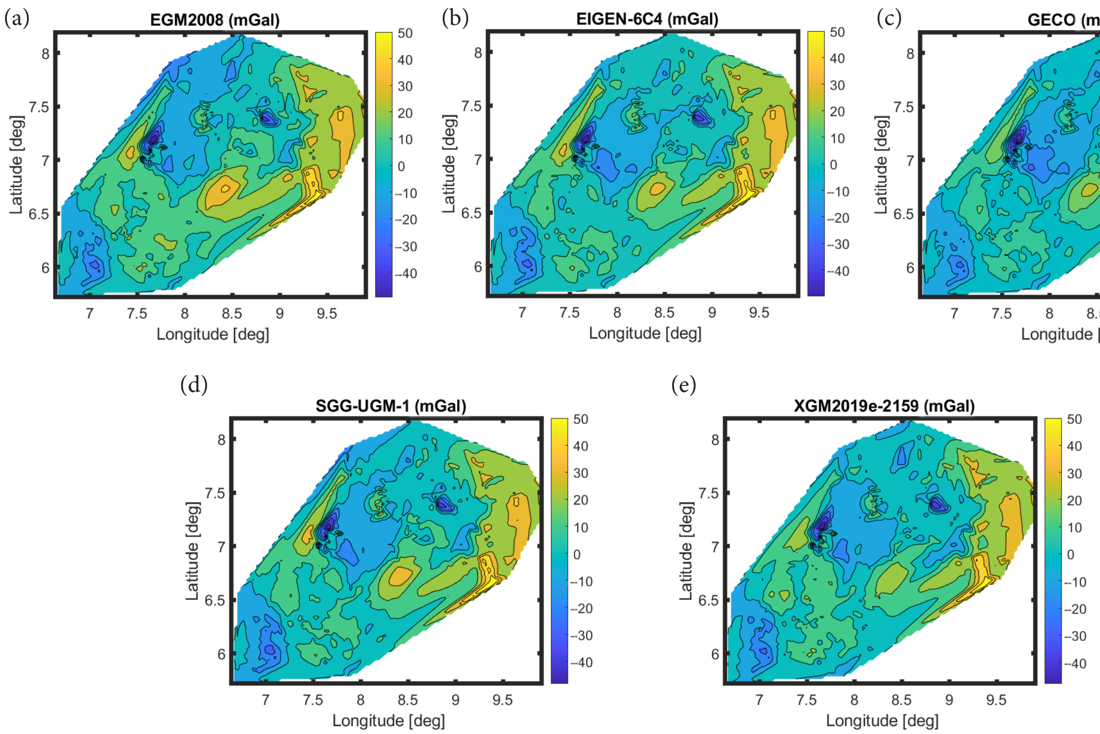

Figure 6. Differences between ground-based and GGM-derived Bouguer gravity anomalies:
a – EGM2008; b – EIGEN-6C4; c – GECO; d – SGG-UGM-1; and e – XGM2019e

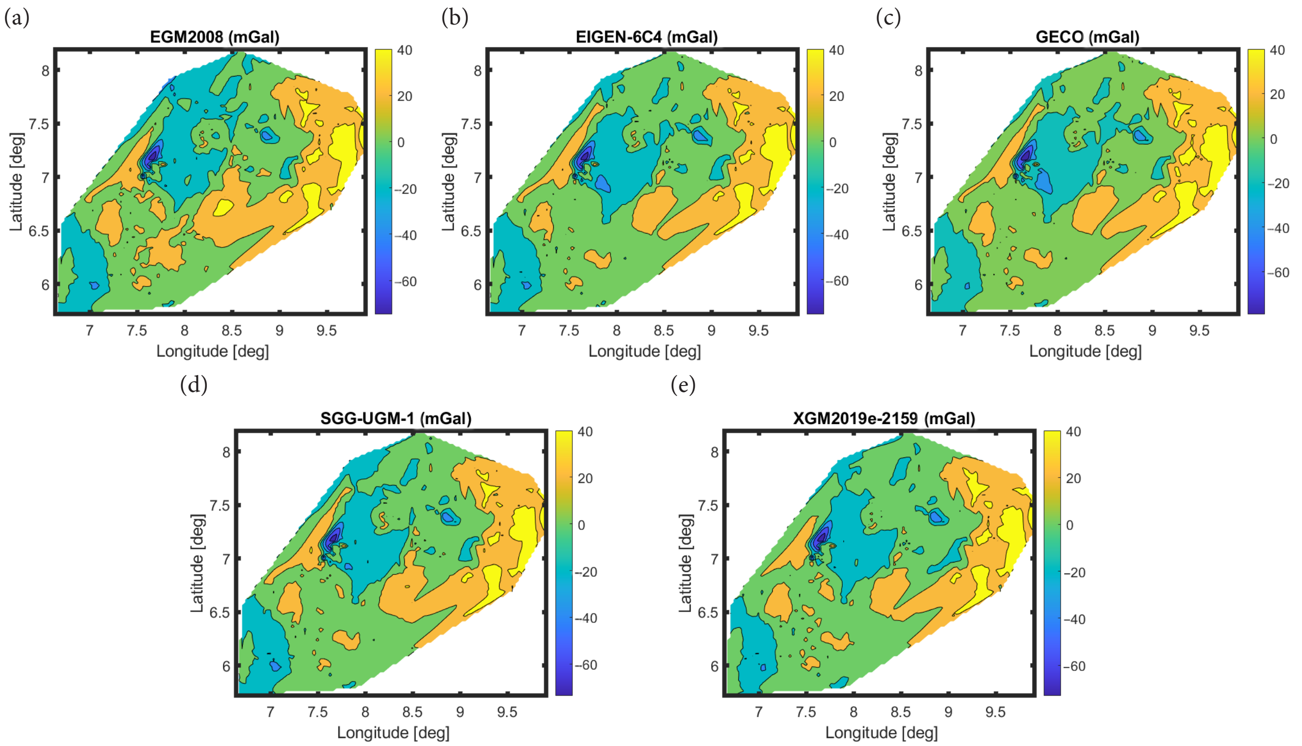

Figure 7. Differences between ground-based and GGM-derived free-air gravity anomalies computed from:
a – EGM2008; b – EIGEN-6C4; c – GECO; d – SGG-UGM-1; and e – XGM2019e

Table 3. Statistics of differences between the ground-based and GGM-derived Bouguer and free-air gravity anomalies

Bouguer Gravity Anomalies (mgal)					
	Min	Max	Mean	STD	RMS
Observed	0.00	0.00	0.00	0.00	0.00
EGM2008	–51.36	53.28	7.35	12.29	14.32
EIGEN-6C4	–53.37	55.26	5.18	11.55	12.65
GECO	–57.10	58.88	5.79	11.75	13.10
SGG-UGM-1	–51.05	55.14	5.71	11.71	13.02
XGM2019e	–49.92	54.28	5.95	11.45	12.90
Free-air Gravity Anomalies (mgal)					
	Min	Max	Mean	STD	RMS
Observed	0.00	0.00	0.00	0.00	0.00
EGM2008	–77.65	56.35	10.42	15.49	18.67
EIGEN-6C4	–79.66	57.43	8.26	14.66	16.82
GECO	–83.36	60.49	8.87	14.93	17.36
SGG-UGM-1	–77.80	56.85	8.82	14.86	17.28
XGM2019e	–76.27	58.05	9.03	14.69	17.24

3.2. Geological interpretation of gravity maps

The digitized geological maps of the Afikpo and Anambra Basins were compared with the interpolated raster surface maps of the five GGMs. We used a cubic interpolation method to produce these maps. We did not change a spatial resolution (or in this case made the classes to conform to the existing geological map) because in many practical cases, geological mapping is to be carried out where there are no existing geological maps. We produced each of the maps on a 5′ × 5′ regular grid. The Bouguer gravity maps are shown in Figures 8 and 9 for the Afikpo and Anambra Basins, respectively. The corresponding gravity gradient maps for both basins are presented in Figures 10 and 11. For the Afikpo Basin, the distinct colour ramp of seven classes was obtained for four (EGM2008, EIGEN-6C4, GECO, SGG-UGM-1) of the GGMs and nine for XGM2019e_2159 from the Bouguer gravity anomalies (see Figures 8a–e). For the Anambra Basin, the distinct color ramp of seven classes was obtained for four (EIGEN-6C4, GECO, SGG-UGM-1, XGM2019e_2159) of the GGMs and nine for EGM2008 from the Bouguer gravity anomalies (see Figures 9a–e).

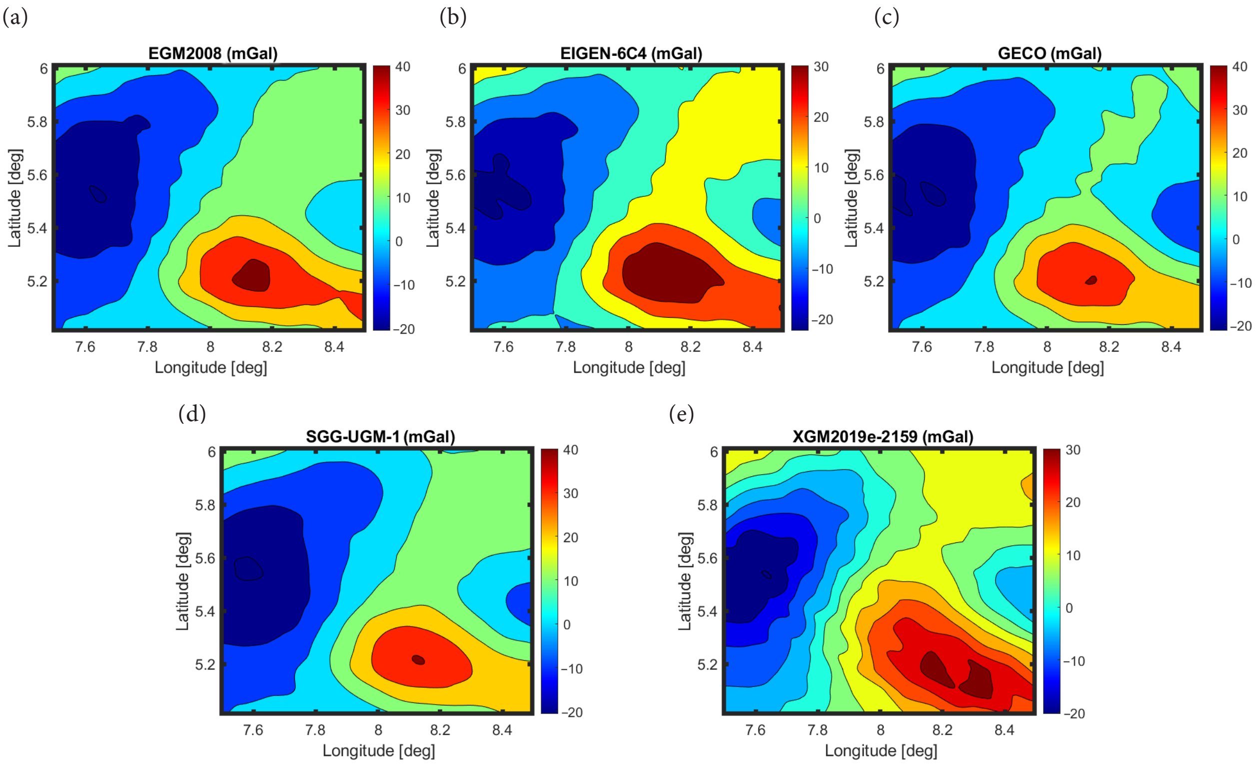

Figure 8. GGM-derived Bouguer gravity map of the Afikpo Basin:
a – EGM2008; b – EIGEN-6C4; c – GECO; d – SGG-UGM-1; and e – XGM2019e

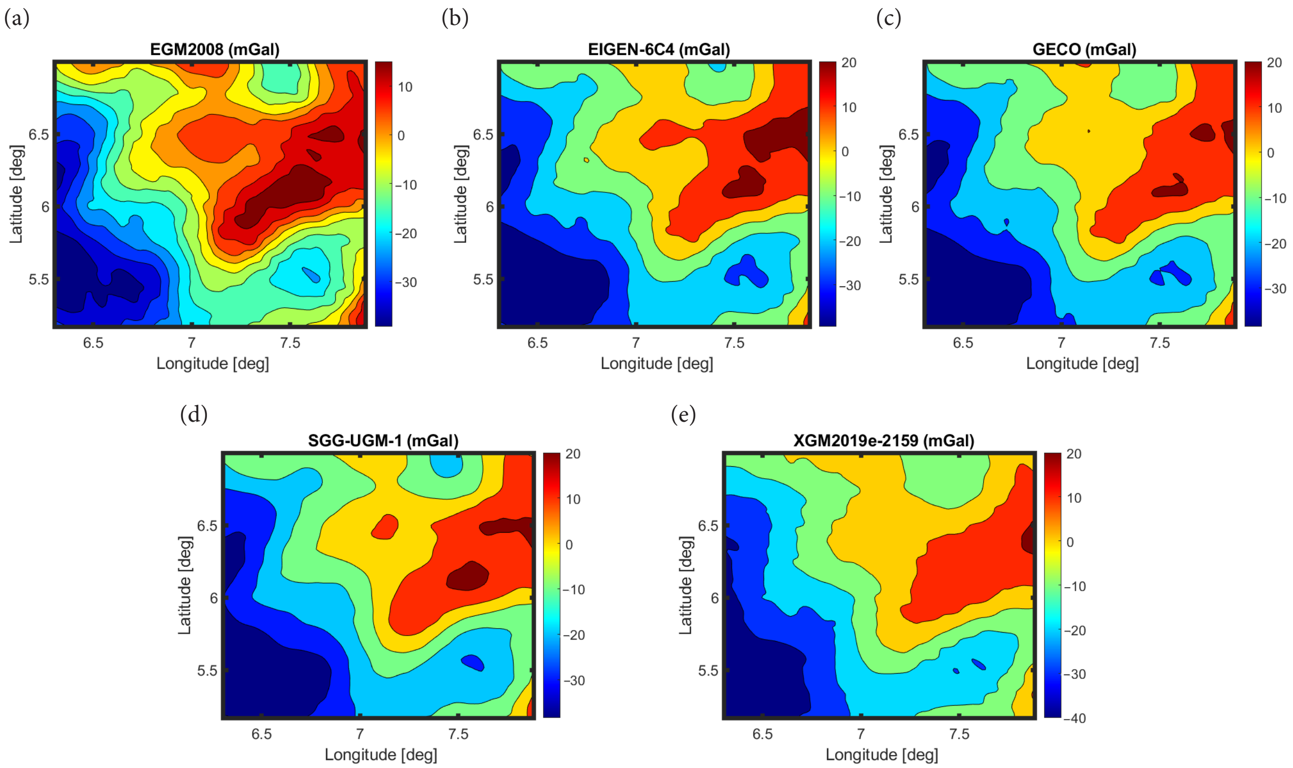

Figure 9. GGM-derived Bouguer gravity map of the Anambra Basin:
a – EGM2008; b – EIGEN-6C4; c – GECO; d – SGG-UGM-1; and e – XGM2019e

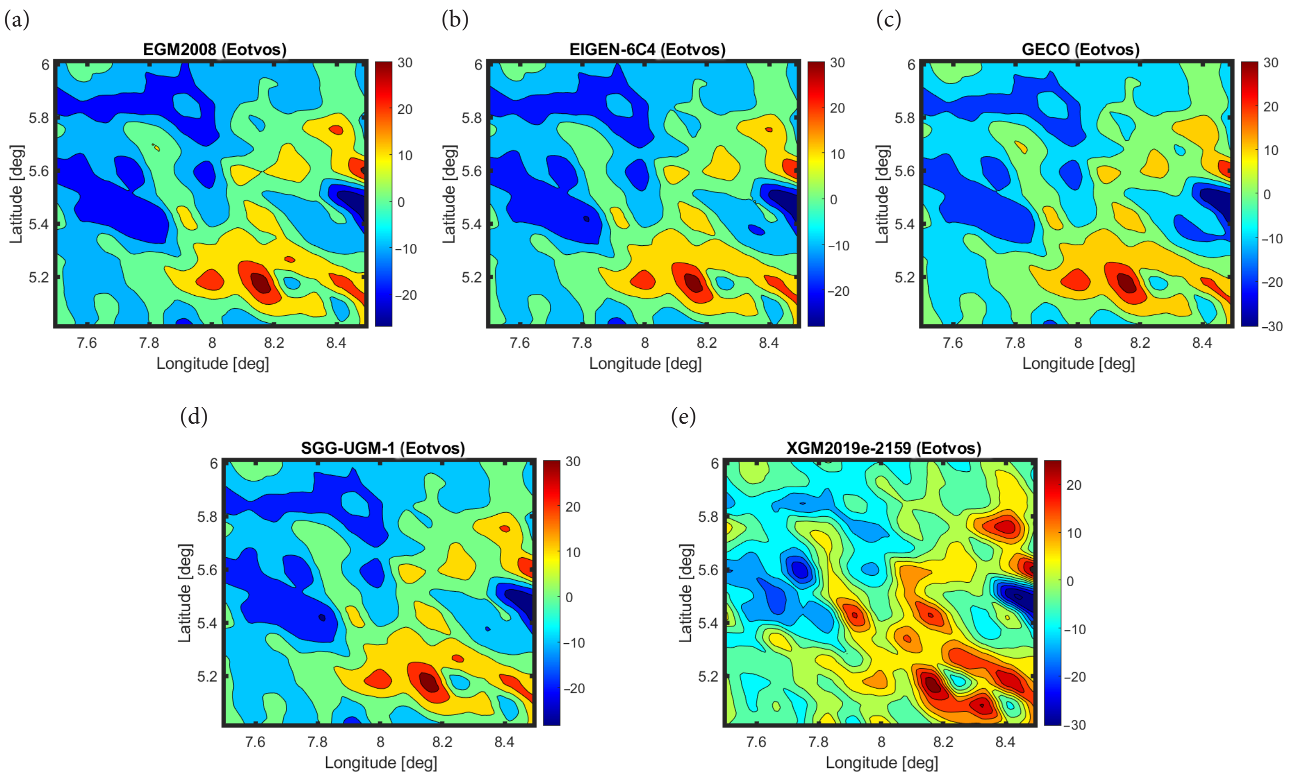

Figure 10. GGM-derived gravity gradient map of the Afikpo Basin computed from:
a – EGM2008; b – EIGEN-6C4; c – GECO; d – SGG-UGM-1; and e – XGM2019e

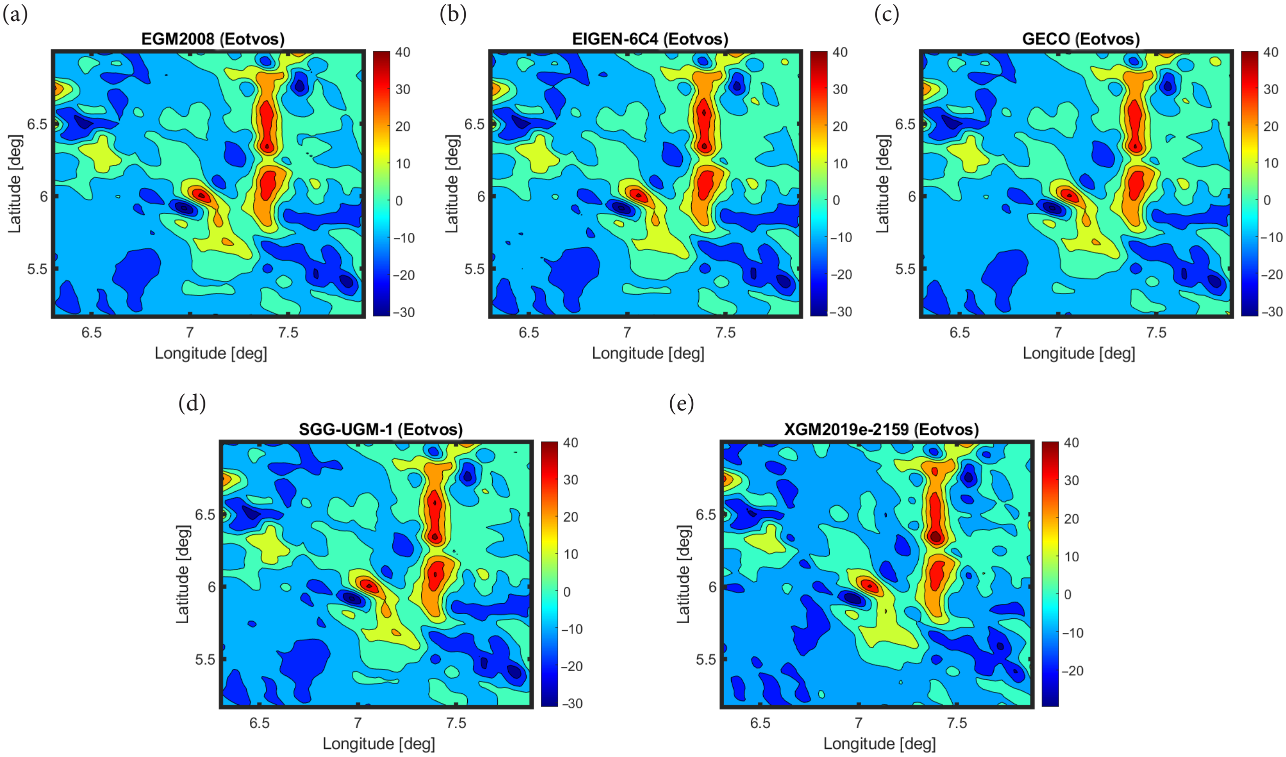

Figure 11. GGM-derived gravity gradient map of the Anambra Basin computed from: a – EGM2008; b – EIGEN-6C4; c – GECO; d – SGG-UGM-1; and e – XGM2019e

4. Discussion

In this section, we interpret the results presented in Section 4, and discuss major findings. We first compare gravity maps and then interpret them in the context of geological and tectonic configuration of the Afikpo and Anambra Basins.

4.1. GGM-derived and ground-based gravity maps

The statistical summaries in Section 4 indicate that more recently developed GGMs generally better agree with the ground-based gravity measurements. The range of differences between each of GGMs and ground-based gravity data can be seen in Tables 2 and 3.

Table 2 relates to the internal consistency of the ground-based and GGM-derived gravity field quantities (Bouguer and free-air gravity anomalies) while Table 3 shows their external consistencies. Obviously, the ground-based gravity measurements were taken as the standard for our comparison. Considering the mean values, we can see a systematic bias of about 5 mgal in four (EIGEN-6C4, GECO, SGG-UGM-1, XGM2019e) of the GGM-derived Bouguer gravity anomalies and about 7 mgal in EGM2008 (see Table 2). Similarly, we can see a systematic bias of about 8 mgal in these four GGM-derived Bouguer gravity anomalies and about 10 mgal in EGM2008 (see Table 2). Existence of these systematic inconsistencies may be due to a topographic bias arising from a truncation of the ETOPO1 topographic model used in the GGMs (Barthelmes, 2013; Barthelmes & Köhler, 2016; Ince et al., 2019), errors in the ETOPO1 model and uncertainties of altimeter-derived topographic heights for ground-based gravity sites. We see also relatively large RMS of differences between the ground-based and GGM-derived gravity data. These systematic and more localized discrepancies might also be attributed to density heterogeneities within the lithosphere as well as errors in gravity values computed using the terrain model for a chosen constant value of topographic density. It is a common knowledge that there are always deviations in gradient of the undulating terrain when point values are compared to mean values obtained from Digital Elevation Models (DEMs) such as ETOPO1.

As seen in statistical summaries of differences between the ground-based and GGM-derived gravity data in Tables 2 and 3, the EIGEN-6C4 model has a better fit with the ground-based gravity data in terms of the RMS of their differences. This is possibly due to using more ground-based gravity data from the study area to compile this model. We note that the XGM2019e model has a very similar RMS fit with ground-based gravity data as the EIGEN-6C4 model. This is explained by involving the topographic information in the development of this model to recover a gravitational signature of topographic relief. This is also apparent from the spatial gravity pattern in maps shown in Figures 4–7.

As seen in Tables 2 and 3, there is a noticeable improvement in more recent versions of EGM2008 (GECO and SGG-UGM-1). The addition of GOCE satellite data as well as other corrections (cf. Gilardoni et al., 2016; Liang, 2018; Xu et al., 2017) to EGM2008 significantly improved their regional fit with ground-based gravity measurements. This justifies the need for assessment of GGMs and substantiates the necessity of tailoring already existing GGMs to fit applications in geosciences.

4.1.1. Tailored GGM-derived gravity data

Following our observation of a systematic bias between the ground-based and GGM-derived gravity field quantities (for the free-air and Bouguer gravity anomalies), we tailored the GGM-derived values by removing a systematic bias in the Bouguer gravity anomalies. Similarly, we removed a systematic bias in the free-air gravity anomalies. The resulting statistical values are summarized in Tables 4 and 5. As seen in Table 5, there is a very close similarity in the RMS values of four GGMs except for EGM2008. The improvement of external consistency with the ground-based gravity anomalies underscores the importance of tailoring GGMs to fit locally or regionally measured gravity data.

4.2. Geological interpretation of gravity maps

We could see general similarities between gravity maps computed using investigated GGM models (see Figures 8–11). Spatial patterns in the Bouguer gravity maps generally agree with major geological features of the Afikpo and Anambra Basins (compare Figures 2 and 3 with Figures 8 and 9). The XGM2019e Bouguer gravity map of

Table 4. Statistics of the ground-based and tailored GGM-derived Bouguer and free-air gravity anomalies

Bouguer Gravity Anomalies (mgal)					
	Min	Max	Mean	STD	RMS
Observed	–52.58	43.65	7.17	17.62	0.00
EGM2008	–35.31	28.75	6.78	11.10	0.00
EIGEN-6C4	–41.71	33.39	6.96	13.52	0.00
GECO	–43.32	32.41	6.35	13.13	0.00
SGG-UGM-1	–41.26	31.78	6.43	12.94	0.00
XGM2019e	–36.27	29.66	6.19	12.39	0.00
Free-air Gravity Anomalies (mgal)					
	Min	Max	Mean	STD	RMS
Observed	–33.98	80.18	26.62	23.40	0.00
EGM2008	–14.77	62.08	26.20	14.29	0.00
EIGEN-6C4	–20.08	64.73	26.36	16.39	0.00
GECO	–21.31	62.24	25.75	16.16	0.00
SGG-UGM-1	–18.24	63.04	25.80	15.63	0.00
XGM2019e	–18.60	62.32	25.59	15.39	0.00

Table 5. Statistics of differences between the ground-based and tailored GGM-derived Bouguer and free-air gravity anomalies

Bouguer Gravity Anomalies (mgal)					
	Min	Max	Mean	STD	RMS
Observed	0.00	0.00	0.00	0.00	0.00
EGM2008	–58.36	46.28	0.35	12.29	12.29
EIGEN-6C4	–58.37	50.26	0.18	11.55	11.55
GECO	–62.10	53.89	0.79	11.75	11.78
SGG-UGM-1	–56.05	50.14	0.71	11.71	11.73
XGM2019e	–54.92	49.28	0.95	11.45	11.49
Free-air Gravity Anomalies (mgal)					
	Min	Max	Mean	STD	RMS
Observed	0.00	0.00	0.00	0.00	0.00
EGM2008	–87.65	46.35	0.42	15.49	15.50
EIGEN-6C4	–87.66	49.43	0.26	14.66	14.66
GECO	–91.36	52.49	0.87	14.93	14.96
SGG-UGM-1	–85.80	48.85	0.82	14.86	14.88
XGM2019e	–84.27	50.05	1.03	14.69	14.72

the Afikpo Basin, however, significantly differs from other GGMs. Similarly, we see inconsistencies in the EGM2008 Bouguer gravity map for the Anambra Basin. A closer look at the gravity (and gravity gradient) patterns revealed that there is a close similarity between the GECO (see Figures 8c, 9c, 10c, 11c) and SGG-UGM-1 (see Figures 8d, 9d, 10d, 11d) models. This is explained by the fact that both models were compiled using similar datasets (EGM2008 and GOCE).

We see eight prominent geological formations as delineated in the existing geological maps of the Afikpo Basin (Figure 2) and the Anambra Basin (Figure 3). In comparison with the number of colour ramps, there are mainly seven classes depicted in the five investigated GGMs (see Figures 8a–e and 9a–e). This may be because of the grid size (5’ × 5’) as well as the raster interpolation method (cubic interpolation) used. The EIGEN-6C4 and XGM2019e gravity patterns more closely mimics the geological configuration of both basins (Figures 8 and 9). However, the EGM2008 gravity pattern appears to show more formations in the Anambra Basin than all other models (see Figure 9a). At this point, we must note that the geological formation called the Niger Delta sediments in the Afikpo Basin contains smaller formations as depicted in the Anambra Basin. A good reference point for the comparison of both basins is the Nsukka formation near Umuahia town. As mentioned earlier, the Afikpo Basin is a continuous southeastward extension of the Anambra Basin. It is interesting to note that all GGMs gravity patterns exhibit other smaller formations inside the Niger Delta sediments formation. From the Bouguer gravity maps in Figure 8, the Precambrian basement in the Afikpo Basin is better exhibited in the EGM2008, EIGEN-6C4, SGG-UGM-1 and XGM2019e gravity maps (see Figures 8a, b, d, e). There is a similar gravity image of Alluvium in all GGMs in both basins. These alluvial deposits (clay, silts, sand, and gravel) would have been greatly influenced by the Niger River in the Anambra Basin. Even though some GGMs have a better agreement with ground-based gravity measurements or better mimics some geological features, other features are absent. The use of more than one GGM or gravity sources is thus needed for a comprehensive interpretation of geological features.

The Bouguer gravity maps (see Figures 8 and 9) computed using five GGMs have close similarities with geological maps than the corresponding gravity gradient maps. This close spatial correlation of the Bouguer gravity anomalies with the geological configuration confirms their applicability and interpretability in delineating geological structures. The distorted pattern as observed in the gravity gradient maps (see Figures 10 and 11) is likely due to a high sensitivity of the vertical gravity gradient on the topographic relief that is superimposed over a generally weaker gravitational signature of the upper crustal density structure that reflects geological setting of the study area. One thing that can also be readily seen, as corroborated in previous studies (cf. Pappa et al., 2019; Bouman et al., 2016), is that the vertical gravity gradient sharpens anomalies over shallow crustal density structures and tends to reduce anomaly complexity, thereby allowing clearer imaging of the causative structures. However, uncertainties in GGMs propagate relatively more in the gravity gradient

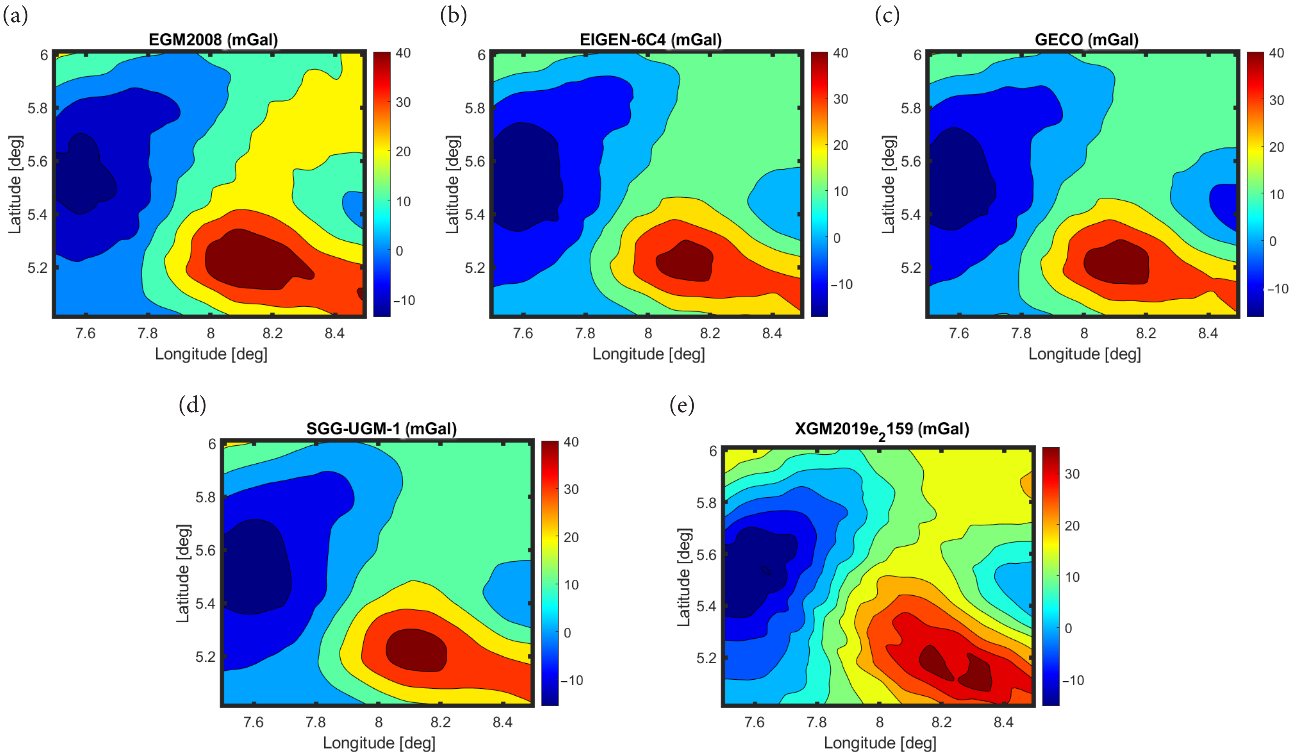

Figure 12. Tailored GGM-derived Bouguer map of the Afikpo Basin:
a – EGM2008; b – EIGEN-6C4; c – GECO; d – SGG-UGM-1; and e – XGM2019e

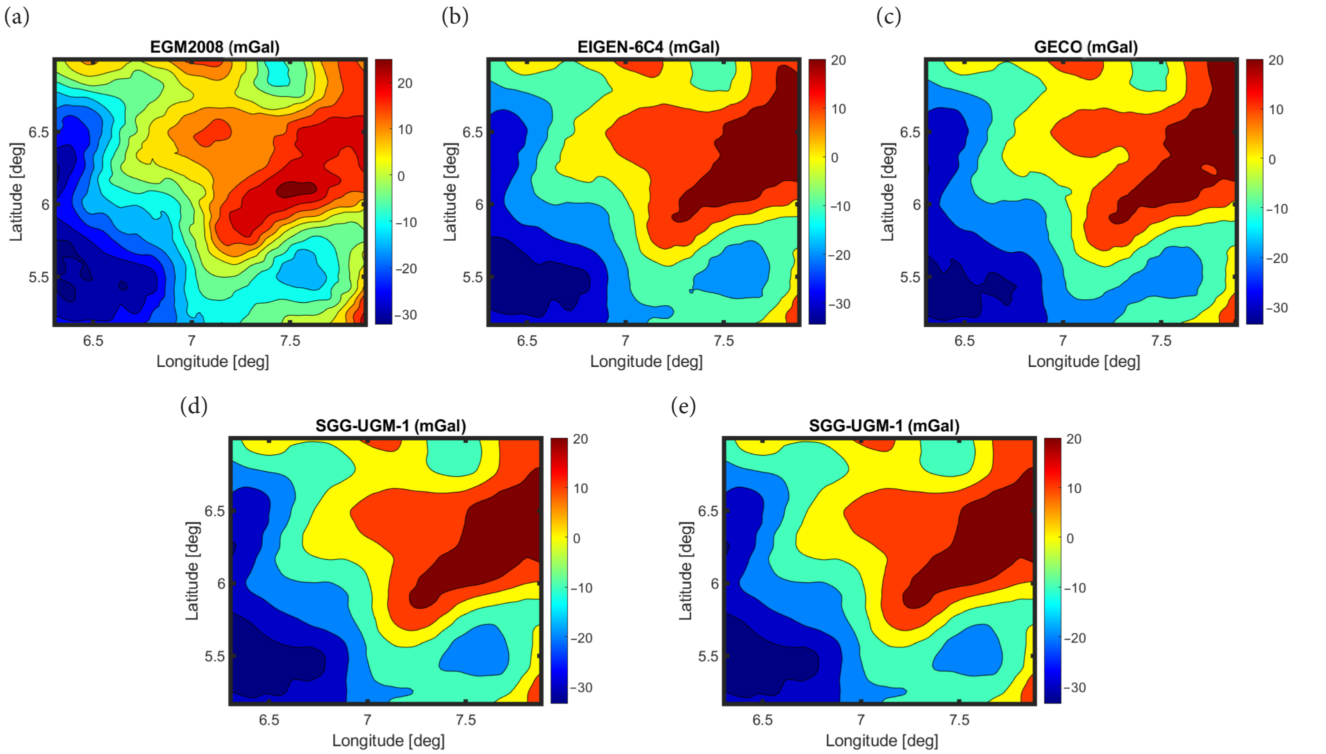

Figure 13. Geological versus tailored GGM-derived Bouguer gravity map of the Anambra Basin:
a – EGM2008; b – EIGEN-6C4; c – GECO; d – SGG-UGM-1; and e –XGM2019e

values (particularly by amplifying at shorter wavelengths) than in gravity values. Consequently, the noise might suppress some more detailed spatial features in the gravity gradient that are otherwise clearly recognized in gravity maps. Nevertheless, the gravity gradient maps provide typically a better image of geological margins rather than an image of geological units, even in the presence of noise.

4.2.1. Tailored GGM-derived Bouguer gravity maps

Interestingly, we can see that after removing a bias in the GGM-derived gravity maps, the EGM2008 gravity pattern closely mimics the gravity pattern of the untailored version of EIGEN-6C4 in the Afikpo Basin. This is also apparent from the statistical summary in Tables 4 and 5. It is worth mentioning that the tailored GECO model was substantially improved as evident from the fact that it more clearly delineates geological features in both basins. We notice that the gravity image of the tailored versions (see Figures 12 and 13) of EIGEN-6C4, GECO and SGG-UGM-1 models are now more closely similar than their untailored versions. This similarity may be occasioned by their sources of data. We also see that the tailored Bouguer gravity maps of all investigated GGMs better depict geological features in both basins than their untailored versions.

Summary and conclusions

We have evaluated the suitability of five combined GGMs using both geological and statistical analyses with the aim to select the most suitable GGM that can be used directly or indirectly, with corrections, for an initial geological mapping of middle belt and Southeastern Nigeria. For this purpose, we digitized geological maps of the Afikpo and Anambra Basins and evaluated geological signatures implied in the Bouguer gravity and gravity gradient maps. We selected these two prominent geological basins around the study area because those basins could serve as a good representation of the geological setting of the whole region. We further used more than 2,900 gravity measurements provided by the Nigeria Geological Survey Agency (NGSA) to assess the accuracy of these GGMs.

The RMS of differences between the ground-based and GGM-derived free-air gravity anomalies range from 14.66 to 15.50 mgal (for all five investigated GGMs). The corresponding RMS of differences in the Bouguer gravity anomalies range from 11.45 to 12.29 mgal. These relatively large differences are partly due to the inherent omission and commission errors in the GGMs and partly also attributed to systematic errors in ground-based gravity data and topographic heights.

We demonstrated that the XGM2019e and EIGEN-6C4 Bouguer gravity maps reproduce better the geological configuration of both basins. We further demonstrated the extent of how topographic errors could adversely affect the accuracy of GGM and underscore the importance of tailoring the existing GGMs to become more suitable for a particular region. We found out that the XGM2019e is the most suitable for geological mapping of this study area. The main reason is that the topographic information was used to reconstruct a higher-degree spectrum of this gravitation model. This is possible, because a higher-degree free-air gravity spectrum is relatively highly spatially correlated with the topographic relief. Nevertheless, this model poorly exhibits some geological features in the Niger Delta sediments of Afikpo basin. A reason might be that the incorporation of the topographic information does not necessarily improve the interpretational quality for geological applications, because it can also suppress some features particularly a gravitational signature of shallow density structures. We recommend that available gravity datasets and any supporting geological, geophysical information should be used for a comprehensive geological interpretation.

The noise in gravity gradient maps suppress more detailed spatial features that are otherwise clearly recognized in gravity maps. Nevertheless, the gravity gradient provides typically a better image of geological margins rather than an image of geological units, even in the presence of noise.

Acknowledgements

Authors are very grateful to the Nigerian Geological Survey Agency (NGSA) for providing terrestrial gravity data for this study.

Author contributions

OIA conceived the study and was responsible for the design and development of the data analysis. OIA and RT were responsible for data collection and analysis. OIA and RT were responsible for data interpretation. OIA wrote the first draft of the manuscript. RT prepared the final version of the manuscript.

Disclosure statement

The authors declare that they have no known competing financial interests or personal relationship that could have appeared to influence the work reported herein.

References

Akaegbobi, M. I. (2005). Sequence stratigraphy of Anambra Basin. *Journal of African Earth Sciences*, *42*, 394–406.

Amajor, L. C. (1987). Paleocurrent, petrography and provenance analysis of the Ajali Sandstone (Upper Cretaceous), south Benue Trough, Nigeria. *Sedimentary Geology*, *54*, 47–60. https://doi.org/10.1016/0037-0738(87)90003-0

Anakwuba, E. K., Ajaegwu, N. E., Ejeke, C. F., Onyekwelu, C. U., & Chinwuko, A. I. (2018). Sequence stratigraphic interpretation of parts of Anambra Basin, Nigeria using geophysical well logs and biostratigraphic data. *Journal of African Earth Sciences*, *139*, 330–340. https://doi.org/10.1016/j.jafrearsci.2017.12.018

Andersen, O., Knudsen, P., & Stenseng, L. (2015). The DTU13 MSS (Mean Sea Surface) and MDT (Mean Dynamic Topography) from 20 years of satellite altimetry. In S. Jin, R. Barzaghi (Eds.), *International Association of Geodesy Symposia: Vol. 144. IGFS 2014* (pp. 111–121). Springer. https://doi.org/10.1007/1345_2015_182

Apeh, O. I., Moka, E. C., & Uzodinma, V. N. (2018). Evaluation of gravity data derived from global gravity field models using terrestrial gravity data in Enugu State, Nigeria. *Journal of Geodetic Science*, *8*(1), 145–153. https://doi.org/10.1515/jogs-2018-0015

Bagherbandi, M., & Sjöberg, L. E. (2013). Improving gravimetric–isostatic models of crustal depth by correcting for non-isostatic effects and using CRUST2. 0. *Earth-Science Reviews*, *117*, 29–39. https://doi.org/10.1016/j.earscirev.2012.12.002

Barthelmes, F., & Köhler, W. (2016). The Geodesists Handbook 2016. *Journal of Geodesy*, *90*(10), 907–1205. https://doi.org/10.1007/s00190-016-0948-z

Barthelmes, F. (2013). *Definition of functionals of the geopotential and their calculation from spherical harmonic models: Theory and formulas used by the calculation service of the International Centre for Global Earth Models (ICGEM)*, (Scientific Technical Report STR09/02, Revised ed.). Helmholtz-Zentrum Potsdam, GFZ German Research Centre for Geosciences. https://doi.org/10.2312/GFZ.b103-0902-26

Bouman, J., Ebbing, J., Fuchs, M., Sebera, J., Lieb, V., Szwillus, W., Haagmans, R., & Novak, P. (2016). Satellite gravity gradient grids for geophysics. *Scientific Reports*, *6*(1), 21050. https://doi.org/10.1038/srep21050

Brockmann, J. M., Zehentner, N., Höck, E., Pail, R., Loth, I., Mayer-Gürr, T., & Schuh, W. D. (2014). EGM_TIM_RL05: An independent geoid with centimeter accuracy purely based on the GOCE mission. *Geophysical Research Letters*, *41*(22), 8089–8099. https://doi.org/10.1002/2014GL061904

Chen, W., & Tenzer, R. (2017). Moho modeling in spatial domain: A case study under Tibet. *Advances in Space Research*, *59*(12), 2855–2869. https://doi.org/10.1016/j.asr.2017.03.015

Chouhan, A. K., Singh, D., Pal, S. K., & Choudhury, P. (2022). Delineation of subsurface geological fractures in the Cambay rift and surrounding regions of NW India: An integrated approach using satellite derived EIGEN-6C4 gravity data. *Geocarto International*, *37*(1), 268–283. https://doi.org/10.1080/10106049.2020.1716395

Cratchley, C. R., & Jones, J. P. (1965). *An interpretation of the geology and gravity anomalies of The Benue Valley, Nigeria*. Overseas Geological Surveys.

Dogru, F., Pamukcu, O., Gonenc, T., & Yildiz, H. (2018). Lithospheric structure of western Anatolia and the Aegean Sea using GOCE-based gravity field models. *Bollettino di Geofisica Teorica ed Applicata*, *59*(2).

Drinkwater, M. R., Floberghagen, R., Haagmans, R., Muzi, D., & Popescu, A. (2003). GOCE: ESA's first earth explorer core mission. In G. Beutler, M. R. Drinkwater, R. Rummel, & R. Von Steiger (Eds.), *Earth gravity field from space-from sensors to earth science* (pp. 419–432). Springer. https://doi.org/10.1007/978-94-017-1333-7_36

Ekwere, A. S., Edet, A. E., & Ekwere, S. J. (2012). Groundwater chemistry of the oban Massif, south-eastern Nigeria. *Revista Ambiente & Água*, *7*(1), 51–66. https://doi.org/10.4136/ambi-agua.812

Floberghagen, R., Fehringer, M., Lamarre, D., Muzi, D., Frommknecht, B., Steiger, C., Piñeiro, J., & da Costa, A. (2011). Mission design, operation and exploitation of the gravity field and steady-state ocean circulation explorer mission. *Journal of Geodesy*, *85*(11), 749–758. https://doi.org/10.1007/s00190-011-0498-3

Förste, C., Bruinsma, S. L., Abrikosov, O., Lemoine, J. M., Marty, J. C., Flechtner, F., Balmino, G., Barthelmes, F., & Biancale, R. (2014). *EIGEN-6C4 The latest combined global gravity field model including GOCE data up to degree and order 2190 of GFZ Potsdam and GRGS Toulouse*. GFZ Data Services. https://doi.org/10.5880/icgem.2015.1

Ghomsi, F. E. K., Sévérin, N., Mandal, A., Nyam, F. E. A., Tenzer, R., Kamga, A. P. T., & Nouayou, R. (2020). Cameroon's crustal configuration from global gravity and topographic models and seismic data. *Journal of African Earth Sciences*, *161*, 103657. https://doi.org/10.1016/j.jafrearsci.2019.103657

Gilardoni, M., Reguzzoni, M., & Sampietro, D. (2016). GECO: a global gravity model by locally combining GOCE data and EGM2008. *Studia Geophysica et Geodaetica*, *60*(2), 228–247. https://doi.org/10.1007/s11200-015-1114-4

Hirt, C., Rexer, M., Scheinert, M. Pail, R., Claessens, S., & Holmes, S. (2016). A new degree-2190 (10 km resolution) gravity field model for Antarctica developed from GRACE, GOCE and Bedmap2 data. *Journal of Geodesy*, *90*, 105–127. https://doi.org/10.1007/s00190-015-0857-6

Hirt, C., & Rexer, M. (2015). Earth2014: 1 arc-min shape, topography, bedrock, and ice-sheet models – Available as gridded data and degree-10,800 spherical harmonics. *International Journal of Applied Earth Observation and Geoinformation*, *39*, 103–112. https://doi.org/10.1016/j.jag.2015.03.001

Igwe, O., Okechukwu, N., & Adepehin, E. J. (2013). Assesment of asbestos waste dumpsite in Enugu Metropolis, South-Easthern Nigeria: implications for environmental concern. *Nigeria Journal of Education, Health and Technology Research (NJEHETR)*, *4*(4), 146–158.

Ince, E. S., Barthelmes, F., Reißland, S., Elger, K., Förste, C., Flechtner, F., & Schuh, H. (2019). ICGEM–15 years of successful collection and distribution of global gravitational models, associated services and future plans. *Earth System Science Data*, *11*, 647–674. https://doi.org/10.5194/essd-11-647-2019

Kvas, A., Mayer-Gürr, T., Krauss, S., Brockmann, J. M., Schubert, T., Schuh, W.-D., Pail, R., Gruber, T., Jäggi, A., & Meyer, U. (2019). The satellite-only gravity field model GOCO06s [Data set]. GFZ Data Services. https://doi.org/10.5880/icgem.2019.002

Liang, W. (2018). *SGG-UGM-1: the high-resolution gravity field model based on the EGM2008 derived gravity anomalies and the SGG and SST data of GOCE satellite*. GFZ Data Services. https://doi.org/10.5880/icgem.2018.001

Mayer-Gurr, T. (2007, October 15–17). *ITG-Grace03s: The latest GRACE gravity field solution computed in Bonn* [Conference presentation]. Joint International GSTM and SPP Symposium, Potsdam, Germany.

Morelli, C., Gantar, C., McConnell, R. K., Szabo, B., & Uotila, U. (1972). *The international gravity standardization net 1971 (IGSN 71)*. Osservatorio Geofisico Sperimentale Trieste, Italy.

Nigerian Geological Survey Agency. (2017). *Regional gravity survey of Enugu State*. https://ngsa.gov.ng/regional-gravity-survey-of-enugu-state/

Nigerian Geological Survey Agency. (2012). *List of Geological Sheet Maps*. http://ngsa.gov.ng/wp-content/uploads/2019/11/List-of-Geological-Sheet-Maps-1-100000.pdf

Nwajide, C. S. (2013). *Geology of Nigeria's Sedimentary Basins*. CSS bookshops limited, Lagos.

Obi, G. C., Okogbue, C. O., & Nwajide, C. S. (2001). Evolution of the Enugu Cuesta: a tectonically driven erosional process. *Global Journal of Pure Applied Sciences*, *7*(2), 321–330. https://doi.org/10.4314/gjpas.v7i2.16251

Odera, P. A. (2020). Evaluation of the recent high-degree combined global gravity-field models for geoid modelling over Kenya. *Geodesy and Cartography*, *46*(2), 48–54. https://doi.org/10.3846/gac.2020.10453

Okoro, A. U., & Igwe, E. O. (2018). Lithostratigraphic characterization of the Upper Campanian–Maastrichtian succession in the Afikpo Sub-basin, southern Anambra Basin, Nigeria. *Journal of African Earth Sciences*, *147*, 178–189. https://doi.org/10.1016/j.jafrearsci.2018.06.021

Osazuwa, I. B. (1986). *The establishment of a primary gravity Network for Nigeria* [PhD thesis]. Ahmadu Bello University, Zaria, Nigeria.

Osazuwa, I. B. (1992). The Nigerian standard gravimeter calibration line. *Survey Review*, *31*(245), 397–408. https://doi.org/10.1179/sre.1992.31.245.397

Pal, S. K., & Kumar, S. (2019). Subsurface structural mapping using EIGEN6C4 data over Bundelkhand craton and surroundings: An appraisal on kimberlite/lamproite emplacement. *Journal of the Geological Society of India*, *94*(2), 188–196. https://doi.org/10.1007/s12594-019-1288-4

Pal, S. K., Majumdar, T. J., Pathak, V. K., Narayan, S., Kumar, U., & Goswami, O. P. (2016). Utilization of high-resolution EGM2008 gravity data for geological exploration over the Singhbhum-Orissa Craton, India. *Geocarto International*, *31*(7), 783–802. https://doi.org/10.1080/10106049.2015.1076064

Pappa, F., Ebbing, J., Ferraccioli, F., & van der Wal, W. (2019). Modeling satellite gravity gradient data to derive density, temperature, and viscosity structure of the Antarctic lithosphere. *Journal of Geophysical Research: Solid Earth*, *124*(11), 12053–12076. https://doi.org/10.1029/2019JB017997

Pavlis, N. K., Holmes, S. A., Kenyon, S. C., & Factor, J. K. (2012). The development and evaluation of the Earth Gravitational Model 2008 (EGM2008). *Journal of Geophysical Research: Solid Earth*, *117*(B4). https://doi.org/10.1029/2011JB008916

Pavlis, N. K. (2006, June 19–23). *Global gravitational modeling, an overview considering current and future dedicated gravity mapping missions* [Conference presentation]. IGes Geoid School 2006, The Determination and Use of the Geoid, University of Copenhagen, Denmark.

Rathnayake, S., & Tenzer, R. (2019). Interpretation of the lithospheric structure beneath the Indian Ocean from gravity gradient data. *Journal of Asian Earth Sciences*, *183*, 103934. https://doi.org/10.1016/j.jseaes.2019.103934

Rathnayake, S., Tenzer, R., Pitoňák, M., & Novák, P. (2020). Effect of the lateral topographic density distribution on interpretational properties of Bouguer gravity maps. *Geophysical Journal International*, *220*(2), 892–909. https://doi.org/10.1093/gji/ggz484

Reyment, R. A. (1965). *Aspects of the geology of Nigeria: the stratigraphy of the Cretaceous and Cenozoic deposits*. Ibadan University Press.

Xu, X., Zhao, Y., Reubelt, T., & Tenzer, R. (2017). A GOCE only gravity model GOSG01S and the validation of GOCE related satellite gravity models. *Geodesy and Geodynamics*, *8*(4), 260–272. https://doi.org/10.1016/j.geog.2017.03.013

Yilmaz, M., Yilmaz, I., & Uysal, M. (2018). The evaluation of gravity anomalies based on global models by land gravity data. *International Journal of Geological and Environmental Engineering*, *12*(11), 814–820.

Zingerle, P., Pail, R., Gruber T., & Oikonomidou, X. (2019). *The experimental gravity field model XGM2019e*. GFZ Data Servicer. https://doi.org/10.5880/ICGEM.2019.007